

# Using Game Controller as Position Tracking Sensor for 3D Freehand Ultrasound Imaging

Chan Vei Siang · Farhan Mohamed · Yusman Azimi Yusoff ·  
Dyah Ekashanti Octorina Dewi · Alfiera Anuar · Mohamad Amir Shamsudin ·  
Mong Wey Sheng

Received: date / Accepted: date

**Abstract** The study aims to investigate the feasibility of game controller (i.e., PlayStation Move) to perform as position tracker and to design its implementation of 2D to freehand 3D ultrasound (US) imaging. Position tracking has been widely used in medical applications, especially in imaging navigation. Its use in 2D to 3D US imaging has transformed the slice view limitation into higher dimension data with bigger clinical impacts. As game controller sensors may produce positional and orientation information, it is potential to upgrade their functional capabilities to generate a low-cost and portable position tracker for US imaging. The study consisted of acquisition from game controller sensors, position tracker and US imaging synchronization, and 2D to 3D reconstruction. The position tracker acquisition was accomplished by extracting and fusing signals from accelerometer, gyroscope and magnetometer sensors to obtain positional and orientation data. Quaternion method was used to coordinate the positions and orientations by relating the number theory and algebra. It was preferred due to its stability and efficiency in solving gimbal lock problem. The synchronization was performed by combining acquisition of both systems in the same movement and time. The synchronized data was further reconstructed to produce 3D US volume. Our experiments included game controller position tracker testing and 3D US reconstruction implementation on phantom. The results confirmed that the game controller performance was closely aligned with that of robot arm. Also, the 2D to 3D US reconstruction implementation has revealed promising outcomes.

With these features, the function of the currently available 2D US probes can be prospectively improved using game controller position tracker effectively.

**Keywords** Ultrasound · Medical Imaging · 3D Reconstruction · Medical Visualization · 2D Ultrasound Probe · 3D Imaging · Game Controller · Position Tracking

## 1 Introduction

Ultrasound (US) imaging has been widely known for its critical advantages compared to other imaging modalities. It ranges from real time imaging, non radiation exposure, non invasive, affordable cost, to capabilities of measuring many physiological parameters [1]. Vast developments in computer processor technology have enhanced the US imaging functions in terms of imaging quality, accuracy and reliability, effectiveness and convenience, portability and durability. Its applications also have expanded following the medical demands, not only for diagnostic per se, but also for treatment and surgical guidance [2].

The advancements of conventional two-dimensional ultrasound (2DUS) probe have provided excellent tomographic image of the object, enabling for easier understanding of pathological interpretation and obtaining a mentally impression of volumetric three dimensional (3D) anatomy of the scanned object by merely sweeping the 2D probe along the surface [3]. However, volumetric quantitative analysis and visualization cannot be obtained through this way, especially for large and long objects. Additionally, precise probe localization may be more difficult due to lack of full volumetric view of the object [4,5].

Chan Vei Siang  
Faculty of Computing, Universiti Teknologi Malaysia  
Tel.: +6017-962-0885  
Fax: -  
E-mail: chanveisiang@hotmail.my

Reconstruction from 2DUS frames to three dimensional ultrasound (3DUS) volume has transformed the conventional paradigm of image acquisition, analysis, and visualization techniques into more extensive information for various medical applications. Significant improvements in the generation of structural volumetric representation enable for better visualization and more accurate measurement and analysis [6–10]. Some reconstruction techniques, either sensorless [11, 12] or with position tracking sensors [13–16], have been widely developed to accommodate such needs. Yet, as reconstruction technique plays an important role in the accuracy and applicability of the 3DUS volume, determining the most suitable reconstruction technique is crucial.

Nowadays, position tracking sensor technology has largely expanded its applications into medical fields. It is not only for data localization and motion identification, but also for treatment guidance in intervention and surgery [17–19]. Due to its basic capability of acquiring 3D position and orientation information, it has a vital role in reconstructing the 2DUS frames into 3DUS volume. Still, as many position tracking sensors are available, defining the best one strongly depends on the needs and capacities.

The idea of using game mechanics in solving problems and engaging audience can be seen in many scientific works such as in [20]. In the same time, advanced and consumer friendly hardware technologies have been introduced in game industry to support the ever-increasing demands in producing better gaming experience. These technologies have becoming the cost-effective alternatives in developing solutions for many other applications such as the use of Microsoft Kinect in health [21], retail [22] and entertainment industries [23].

The use of Sonys PlayStation (PS) Move and PS Eye are also proven to be useful in tracking positions in 3D space [24]. In this study, we investigate the use of the visual guided mechanism of PS Move and PS Eye for ultrasound 3D position tracking by using a conventional 2D ultrasound probe.

Most of the researchers focused on attach a sensor with the ultrasound probe, which is good in maintaining the ultrasound probe design. One of the problem lack with embedded sensor is its compatibility with other type of ultrasound probe. Embedded sensor already calibrated with its ultrasound probe and might not be able to be used with another ultrasound probe [25]. This problem has been analyzed in order to ensure the proposed system is compatible with most of the ultrasound probe. The system comes out with a novel mounting mechanism to allow tracking sensors to be fitted with an ultrasound probe. The mounting mechanism can be adjusted to allow tracking sensors to be used with dif-

ferent type of ultrasound probe which makes it compatible with most of the ultrasound probe. The sensor also can be calibrated according to the attached ultrasound probe so the captured 2D images can be positioned accurately.

Another novel improvement is the introduction of 2D ultrasound tracking using optical position tracking which is lacking in current position tracker [26, 27]. Although magnetic sensor able to provide accurate position data, it cannot be placed near to metal-based materials since it may disturb and affect the position information. On the other hands, the optical tracking method uses an image processing algorithm to track ultrasound probe position based on PS Move sphere bulb. The light produced by the bulb can be changed based on the environment in order to get best position tracking experience.

## 2 Methodology

### 2.1 Overview of Position Tracking in Ultrasound Imaging

Due to its high accuracy and application expansion in clinical fields, the use of position tracking sensors in US imaging has expanded from image reconstruction to imaging navigation [17–19]. Although sensorless reconstruction techniques do not require position tracking sensors [11, 12], imaging navigation always necessitates the position tracking sensors. Position tracking based-techniques employ mechanical and freehand scanning techniques [3, 5, 6, 15, 16]. The mechanical technique sweeps the region of interest by mounting the probe to a stepper motor to move the probe in a predefined manner where the relative position and angulation of each frame can be determined precisely. Although mechanical technique has more precise position, it has less probe manoeuvre flexibility. Conversely, the freehand scanning acquires the region of interests by mounting a position tracking system to the probe. Therefore, the freehand scanning technique can be a good choice to obtain the 3D volume due to its flexibility to reach the whole region, even in uneven surfaces. In the freehand system, the scanning geometry is not predetermined. However, freehand 3D ultrasound imaging still suffers from an inadequate sampling process that may obscure the visibility of the object features causing inaccuracy in the extraction of the acquired features. The freehand position tracking system is mostly based on optical or electromagnetic sensors [3, 6, 13, 14]. The choice highly depends on the application and algorithm. However, both have their own advantages and drawbacks.



Fig. 1 PS Move (left) and PS Eye (Right) are used to track position and orientation

As the main component that plays role in image acquisition and characterization, the US probe instrumentation needs to accommodate image quality aspects in imaging physics [28]. Besides the 2DUS probes, some integrated 3DUS probes with mechanical motor inside have also been widely available [6], enabling for 3DUS imaging much easier. The 3DUS is capable of bridging the 2DUS gaps in term of perception dimensional understanding, accuracy and operator dependency in sweeping the probe, and positional variability. Yet, some physical factors related to 3DUS reconstruction, for instance imaging artefacts due to motions, trajectory accuracy and geometrical distortion, and complexity of the scanning procedure, must be taken into account for optimum results [6]. Additionally, since mechanical motor has its predetermined scanning trajectory and region, the shape of the reconstructed 3DUS volume also follows the pattern of the mechanical motor [6, 14]. In this regard, the flexibility of the probe movement may not be a problem. However, not all US machine is compatible with such probe system. Otherwise, even if it is compatible, the US machine comes from high end and high cost generation [5, 6].

From the clinical applications point of view, a large number of 3DUS applications have been currently produced and widely applied in clinical basis. The techniques have been widely used in obstetrics and gynaecology [29–32], orthopaedics [33, 34], oncology [35, 36], and many more. The implementation is currently not only for computer-aided diagnostics, but also have been transforming for image-guided therapy and surgery.

### 2.1.1 Optical Tracking Method

The optical tracking method mainly relies on the sphere on the top of the PS Move and then tracked by the PS Eye. The Figure 1 shows the PS Move and PS Eye. It contains RGB LED which is able to lid the sphere into different colours. Blob tracking method or specifically circular blob shape tracking is used to track the sphere position from camera image obtained from

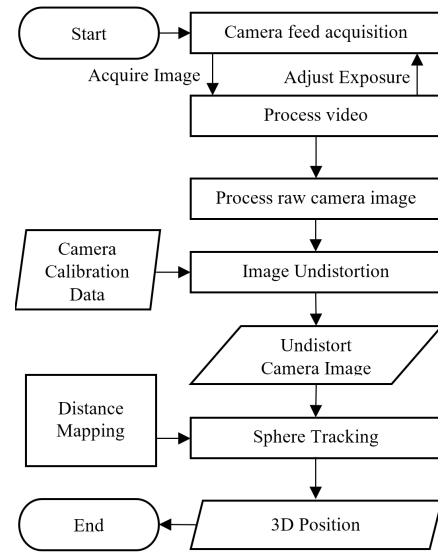


Fig. 2 Flow chart of optical tracking method

PS Eye [37]. The blob tracking produces position in two-dimension as well as radius of the sphere. The position and radius data allow for the PS Move API to map the sphere radius value with depth value, then combine them with acquired position to produce a 3D position. Figure 2 reveals the optical tracking process flowchart.

In order to achieve best tracking capability, there exist four tracking algorithms applied in the PS Move API, which are edge-based sphere tracking, colour-based sphere tracking, mean-shift blob tracking, and sphere-size calculation. The edge-based sphere tracking, as presented in [38], extracts and tracks the sphere outline using 2D Hough Transform. Figure 3 shows the process to acquire position of the circular object. The colour-based sphere tracking, based on the work presented in [39], is implemented in the PS Move API. The colour is used to support the tracking process by filtering the other object in the camera image. The method provides better solution in detecting sphere using HSV colour space. Tracking an object in multi-colour objects in the background also may lead to tracking failure because of the change in the background. Hence, PS Move API uses mean-shift blob tracking with adaptive feature selection and scale adaptation to handle this problem [40]. Scale adaptation is used to handle the changes of the sphere size. Another important result of the method shows that drastic changes in pixel around sphere boundary, making pixel value at the sphere boundary very important to shift the tracking area. Lastly, the algorithm from [41] is also implemented in PS Move API.

Figure 4 displays the flowchart of search algorithm to find the sphere centre point. The sphere-size calculation is used by systematically filling the majority of

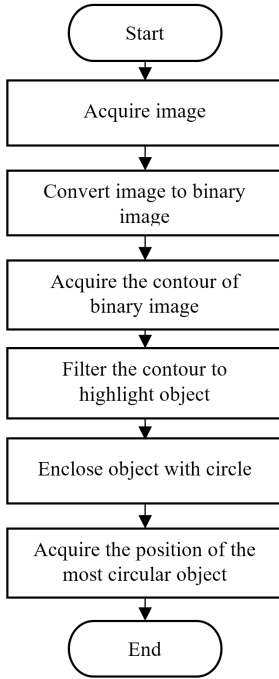


Fig. 3 Flow chart of circular edge detection

the pixel in the colour area. The sphere size is calculated based on the total number of pixels or the pixel area. Afterwards, the depth of the sphere also can be deduced.

### 2.1.2 Orientation Tracking Method

The accelerometer, gyroscope and magnetometer are the three type of sensors that have been embedded inside the PS Move. All sensors function as three-axis sensor in the PS move device. As each sensor has their own advantages and drawback, the sensor data are fused to improve the orientation tracking capabilities. Gyroscope is able to provide quick response in rotation. Accelerometer is able to acquire orientation relative to gravity. Magnetometer is able to obtain orientation based on the magnetic field. The fusing of the information from these three sensors enables to estimate the real orientation of the object in 3D space [37].

The rotations and orientations of the PS Move is saved as the quaternion method [42] in a laptop during the 3DUS reconstruction. A quaternion is a mathematical concept that represent the orientations and rotations of an object in 3D space. Quaternion is used as a descriptive axis direction of rotation and total angle of rotation around the axis [43], as shown in Figure 5. Direction of an axis of rotation and total angle of rotation are represented in (1) to (4):

$$\text{Angle} = \cos(q/2) \quad (1)$$

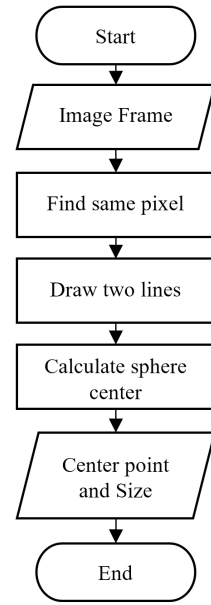


Fig. 4 Flow chart of sphere centre point search algorithm

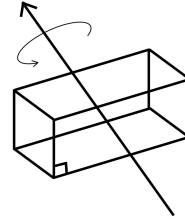


Fig. 5 Direction of axis of rotation and angle of rotation around axis

$$\text{Axisx} = qx / \sqrt{1 - q^2} \quad (2)$$

$$\text{Axisy} = qy / \sqrt{1 - q^2} \quad (3)$$

$$\text{Axisz} = qz / \sqrt{1 - q^2} \quad (4)$$

where the total angle of rotation is known as Angle. The directions of axes of rotation in x, y, and z are denoted as Axisx, Axisy, and Axisz respectively. The quaternion values are represented as qx, qy, and qz

Due to its numerically more stable and efficient characteristics, the quaternion method is chosen. The quaternion method can also avoid the problem of gimbal lock in Euler angle, where the gimbal lock is the loss of one degree offreedom in a three-dimensional because both yaw and roll rotate about the vertical axis [44].

Table 1 Hardware used during experimental setup

Hardware Specification	Model
Ultrasound System	Toshiba Aplio 300
2D Ultrasound Probe	PVT-375 BT 3.5MHz
Computer Monitor	HP L1740, screen resolution 1280 x 1024
Workstation	Alienware m17 x R4 i7 3840QM, 16GB

Table 2 Software required during experimental setup

Software Specification	Software Version / Name
Library	VTK 5.0.1
	PS Move API 3.0
IDE	Visual Studio 2012
Driver	CL Eye Test Driver
	VGA2USB Frame Grabber

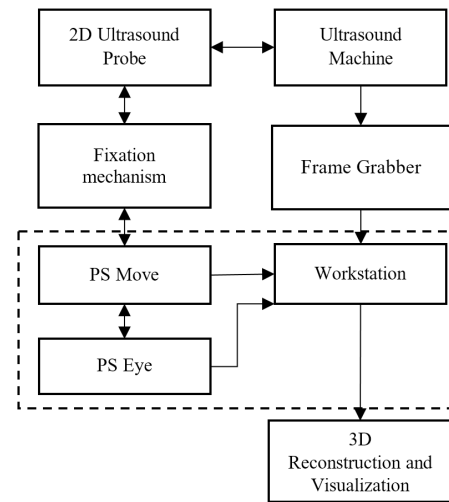


Fig. 6 System design of the tracking and reconstructing 3D visualization

### 2.1.3 Position Tracker and Ultrasound Imaging Synchronization

The synchronization between the position tracker and US imaging is performed in hardware setting and software design. The system requires specific hardware and software lists as given in Table 1 and Table 2.

### 2.2 Hardware Setting

The synchronization hardware involves an ultrasound machine that is connected to a laptop using a frame grabber. Figure 6 describes the overall of the system design. The PS Move is connected to a computer by using Bluetooth communication. The internal sensors of PS Move collect the positions and orientations in a freehand manner. The PS Move is attached to the US probe by using a fixation mechanism which holds both devices and ensures for similar movement. The output display of the US machine can be extended to another monitor. An image grabber is required to extract the output display and show it in the workstation, by converts the output display and view in specially designed software on the workstation.

On the other hand, the PS Eye is connected to a laptop using USB cable in order to acquire the accurate position of the PS Move. A CL eye test driver needs to be installed in a laptop to allow the PS Eye to work in the workstation. The calibration process needs to be carried out before using the PS Move and PS Eye. The magnetometer calibration can be done by rotating PS Move at different directions in front of PS Eye. Light ball on top of the PS Move may change the colour based on the environment in order to get best tracking experience. The colour is selected by identifying the available

colour in the scene with the most contrast colour from list of colour produced by the light ball. The algorithm is implemented in the PS Move API.

### 2.3 Software Design

The software design consists of image acquisition and 3D ultrasound reconstruction.

#### 2.3.1 Image Acquisition

Image acquisition involves the collection of 2DUS images, position and orientation to the workstation for 3D reconstruction. Figure 7 describes the flowchart of image capturing process.

The system captures the screen from the US machine display when the PS Move button is pressed. Then, the system saves the image in bitmap format with `imgi` as the file name, where `i` is the number. Simultaneously, the positions and orientations of `img i` in quaternion mode is saved in a text file for the use of 3D reconstruction later. The synchronization basically can be performed either from an integrated positional sensing device or from an external system. The advantage of this system is a large adaptability for the probe movement in recording the position and orientation for 3DUS reconstruction with less distortions and errors. In this regard, the synchronization is performed externally by matching the saved image and position and orientation line by line.

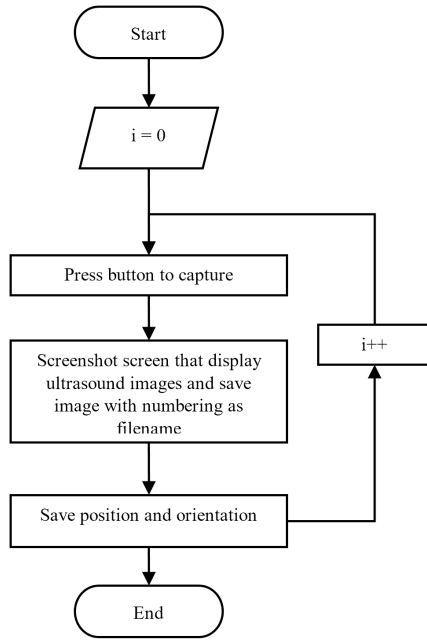


Fig. 7 Flowchart of image capturing process

### 2.3.2 3D Ultrasound Reconstruction

The computational part of the 3DUS reconstruction is in the 2D to 3D volumetric reconstruction algorithm. It aims at building the 3DUS volume using 3DUS reconstruction algorithms based on the synchronized data of position and orientation as well as 2DUS image [16,17,45].

Thus far, various reconstruction techniques have been proposed to obtain the 3DUS volume out of 2DUS probe scanning, either sensorless [11,12] or with position tracking system [13–15]. The sensorless technique seems to be more practical, but the positional accuracy may be different from that of with position tracking system. Additionally, implementation to positional guidance may be lacking. The position tracking-based 3DUS system utilizes position sensors attached to the 2DUS probe and acquires positional information when the probe is swept around the object. Although less practical, this technique is currently preferred due to its expansion capability.

The reconstruction procedure placed the acquired 2DUS frames into the 3DUS volume based on the correlated relative positions. This process depends on the acquisition of the 2DUS frames and the position of each frame. As the key procedure in generating 3DUS volume, defining a suitable volume reconstruction algorithm is dispensable. Various algorithms have been widely implemented. Basically, it can be divided into voxel nearest-neighbour (VNN), pixel nearest-neighbour

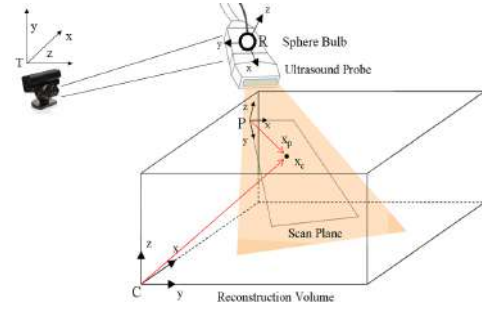


Fig. 8 Bin-filling for 3D ultrasound imaging using optical position and orientation tracker

(PNN), and functional-based methods, such as distance-weighted (DW) interpolations [45,46]. Among these three methods, PNN seems to be the simplest.

In general, the PNN algorithm can be divided into bin-filling step and hole-filling step. The bin-filling step, also known as distribution step, involves the extraction and scaling of every acquired pixel in the 2DUS frame. Then, these pixels are combined with any offset values from one of the acquired positional parameters producing calibrated pixel values. For every calibrated pixel value, rotation matrices taken from the acquired positional parameter are applied to obtain a proper orientation and position of the pixels in the 2D image into the matched part of the 3D volume. In this stage, the voxel value in each 3D volume position is updated by the pixel value of the associated 2D image [47].

The hole-filling step simply estimates the values of the empty reconstructed voxels by using interpolation techniques to fill the gaps without missing any information or inducing any noise. Many works have proposed their hole-filling methods [48]. Above all, the choice of the technique is highly influenced by the image characteristics and application. Figure 8 show the illustration of the tracker setup used with 2D ultrasound probe.

The coordinate system mapping from a 2D frame to a 3D volume is defined by:

$$u = tw \quad (5)$$

where  $u$  is the transformed coordinate system in 3D space by apply the transformation matrix  $t$  on the coordinate system  $w$  of the 2DUS frame.

The position information produces a transformation matrix, where the relationship between pixels coordinates in the original 2DUS frame ( $P$ ), sphere bulb ( $R$ ), and the PS Eye ( $T$ ). The reconstructed 3D volume ( $C$ ) voxel coordinate is formulated as:

$$x_C = T_{CT} T_{TR} T_{RP} x_P \quad (6)$$

where  $x_C$  is the resulting voxel location in  $C$ ,  $x_P$  is pixel location in  $P$ .  $T_{RP}$  denotes a transformation through



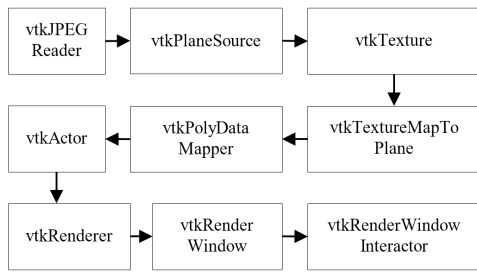


Fig. 9 VTK function used for 3D reconstruction process

the probe calibration from the acquisition coordinates in  $P$  to the associated positional system in  $R$ ,  $T_{TR}$  is the transformation taken directly from the positional system in  $R$  to  $T$ , and  $T_{CT}$  is the positional alignment of  $C$  with  $T$  [47].

### 3D Reconstruction Visualization

Hence, an application is developed to perform 3D reconstruction, which is the core value of the entire research. Visualization Toolkit (VTK) is used to assist the reconstruction process. The VTK is an open-source and free software system for 3D computer graphics, image processing and visualization, and it is widely used for developing medical visualization application. The application reads the saved 2DUS image files, together with the positions and orientations of the images contain in a text file. Next, it generates a plane based on the number of 2D ultrasound image. Then, it will map those images as texture to the plane and arranged it in 3D space. It is important that the position and orientation of every data slice must be accurate to get a precise 3D object. The quaternion method will be used to coordinate the rotations and orientations during the process. Figure 9 shows the flow of the function used in VTK to produce 3D visualization of the aligned images.

## 3 Experimental Setup

### 3.1 Position Tracking Testing

A quantitative testing is conducted to identify the accuracy of the position tracking provided by PS Move and PS Eye in freehand scanning. The test is conducted at a robotic lab where a robot arm is used to move the tracker in a predefined path. Figure 10 show the hardware test setup. PS Eye is place facing the PS Move that is held by the robot. The robot model used in this test is the ABB IRB 120 industrial robots which able to handle a load of 3kg and the movement distance up to 580mm.



Fig. 10 PS Move and PS Eye test setup with ABB industrial robot



Fig. 11 Test setup for capturing 2D ultrasound images and 3D reconstruction process

The robot movement is set up as the ground truth for the test, and the position recorded during the test will be compared with the ground truth. Three different tests are conducted with the purpose to compare the movement of the robot and the freehand in  $x$ ,  $y$  and  $z$  direction. Total distance of the movement is set to 20 cm for each direction. Each test result able to show the tracker sensitivity in other direction while moving in the tested direction. The test only compares the recorded distance and predefined distance of the robot arm. Time is not included in the test as it does not affect the recorded distance.

### 3.2 3DUS Imaging Implementation

A scan session is carried out in implementation phase. The session used a baby phantom to test the capabilities of the 3D ultrasound reconstruction. Figure 11 show

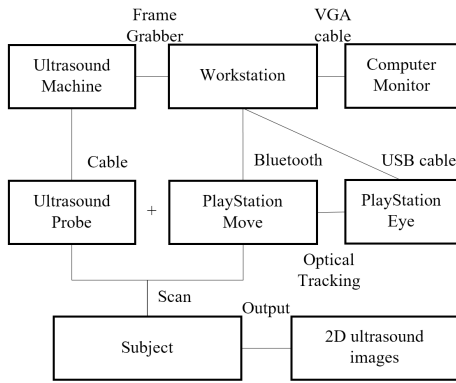


Fig. 12 Connection between devices in the experiment setup from Figure 11

the test setup for capturing 2D ultrasound images and 3D reconstruction process. The output dataset consists a series of 2D ultrasound image frames. The naming convention of each frame is in increasing numerical sequence, such as img0, img1 and so on. Besides that, each frame is accompanied with the respective positions and orientations in text file.

The system is developed in Microsoft Visual Studio 2010 with Visualization Toolkit (VTK). The reconstructed 3D images of the scanned subject are visualized using the VTK libraries. Figure 12 shows the schematic diagram of the research design. Each component has its own connection and operation highlighted using the connector lines.

A comparative study is carried out to compare between the reconstructed result and the real object, based on the different part of subject at a certain position and orientation, such as the head, abdomen and leg. Figure 13 shows the structure of the subject used in this research. The scan direction for both session is different. The session has multiple set of images as captured with its position and orientation. This is because of each image set focus on different part of subject.

## 4 Result and Discussion

### 4.1 Position Tracking Testing Result

Data is successfully saved during testing process. Figure 14 shows part of the position and orientation data saved for every image in a text file. Each line representing the information for an image. A large number of techniques have been used to verify the reliability of the position tracking system in sensing the trajectory. The choice of the technique highly depends on the availability of the testing equipment. Since we consider that robot arm system has high accuracy, we utilize



Fig. 13 Baby phantom acted as subject in the experimental setup as in Figure 11

pos	ori	ori	ori	ori
pos:14.32 18.72 100.73	ori:0.57	-0.58	0.48	-0.35
pos:14.32 18.72 100.73	ori:0.57	-0.58	0.48	-0.34
pos:14.34 18.68 100.64	ori:0.57	-0.58	0.48	-0.34
pos:14.34 18.68 100.64	ori:0.57	-0.58	0.48	-0.35
pos:14.34 18.64 100.60	ori:0.57	-0.58	0.47	-0.35
pos:14.34 18.63 100.56	ori:0.57	-0.58	0.47	-0.35
pos:14.33 18.65 100.62	ori:0.57	-0.58	0.47	-0.35
pos:14.33 18.65 100.62	ori:0.57	-0.58	0.47	-0.35
pos:14.31 18.64 100.67	ori:0.57	-0.58	0.48	-0.35
pos:14.31 18.64 100.67	ori:0.57	-0.58	0.48	-0.35
pos:14.32 18.70 100.74	ori:0.57	-0.57	0.48	-0.35
pos:14.33 18.63 100.68	ori:0.57	-0.58	0.48	-0.35
pos:14.33 18.63 100.68	ori:0.57	-0.58	0.48	-0.35
pos:14.32 18.71 100.76	ori:0.57	-0.58	0.48	-0.35
pos:14.32 18.71 100.76	ori:0.57	-0.58	0.48	-0.35
pos:14.34 18.72 100.80	ori:0.57	-0.57	0.48	-0.35
pos:14.34 18.72 100.80	ori:0.57	-0.57	0.48	-0.35
pos:14.33 18.70 100.83	ori:0.57	-0.57	0.48	-0.35
pos:14.33 18.70 100.83	ori:0.57	-0.57	0.48	-0.35
pos:14.33 18.71 100.84	ori:0.57	-0.57	0.48	-0.35
pos:14.34 18.67 100.85	ori:0.57	-0.57	0.48	-0.35
pos:14.34 18.67 100.85	ori:0.57	-0.57	0.48	-0.35
pos:14.32 18.71 100.89	ori:0.57	-0.57	0.48	-0.35
pos:14.32 18.71 100.89	ori:0.57	-0.57	0.48	-0.35
pos:14.34 18.72 100.84	ori:0.57	-0.57	0.48	-0.35
pos:14.34 18.72 100.84	ori:0.57	-0.57	0.48	-0.35
pos:14.33 18.73 100.84	ori:0.57	-0.57	0.48	-0.35

Fig. 14 Position and orientation data

robot arm system as the trajectory reference and position tracker holder.

Our analysis highlights on the comparison between the reference and the position tracker results. Based on our experimental setting, the results of three movements can be demonstrated in Figure 15.

From the experiment results as shown in the graphs in Figure 15 (A), 15 (B) and 15 (C), we can statistically analyse as follows. In term of correlation analysis, the correlation values of X, Y, and Z axes are 0.9997, 0.9988, and 0.9980. The  $R^2$  values of X, Y, and Z axes are 0.9994, 0.9977, and 0.9961 respectively. While the covariance values of X, Y, and Z axes are 49.1327, 52.6024, and 40.1138 respectively. In term of regression analysis, the slope values for the X, Y, and Z axes are 0.7458, 0.6954, and 0.9105 respectively.

In general, this indicates that our proposed technique is statistically comparable to that of robot arm system. Correlation value measures the extent to which two or more variables fluctuate together. Since the correlation values in our result are close to 1, we can say that the results of our position tracker are almost perfectly close to that of robot arm results. As the  $R^2$



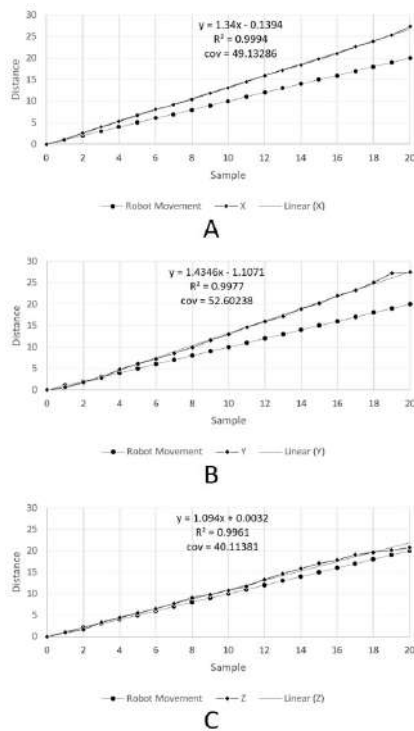


Fig. 15 Comparison of robot movement with recorded position for (A) x-direction, (B) y-direction and (C) z-direction

represents the goodness-of-fit of the test, we can confirm that the values are highly close to the fitted regression line. As the covariance of the two variables in data sample are actually normalized correlation and measures how the two are linearly related, we can see that the covariance values of our position tracker are linearly related. The slope or the gradient of the line, as a number that describes both the direction and the steepness of the line, may indicate an important tendency, as it confirms the degree. All axes have shown considerably high degrees. In addition, the slope in Z-axes reaches the highest among all.

## 4.2 3D Reconstruction Result

The input of 3D reconstruction process is the 2D ultrasound images of baby phantom that are acquired from the ultrasound machine and stored into a laptop. Besides that, the dataset of different position and orientation of the corresponding images are also needed to produce a good visualization of the 3D image reconstruction. The images are made up of only thin slices that provide flatter and low-resolution images. The 2D ultrasound scan provides the outlines and flat-looking images of the scanned anatomy, which are difficult to

understand and analyse for people who are not familiar with 2D ultrasound imaging.

The 2D freehand ultrasound scanning is easy and simple to conduct as user can sweep the probe manually over the baby phantom while a focused image is displayed on the ultrasound machine. At the same time, the image is stream to a workstation using frame grabber. The 2D freehand ultrasound scan can be conducted even for user that has basic experience and skills. The output of the scanning session is a series of 2D ultrasound image that contain a certain part of the baby phantom at a certain position and angle. Figure 16 shows the output of the 2D ultrasound image saved in the workstation. Each image able to capture part of baby phantom structure. The process is repeated 3 time with different focus area which are the head, abdomen and leg.

The 3D ultrasound reconstruction is involved by collect a series of 2D ultrasound images with its corresponding position and orientation, and put them into 3D reconstruction software to obtain 3D images. The 3D ultrasound image is easier to understand because it produces a 3D impression of the scanned object. Therefore, the accuracy of the position and orientation is important for the 3D reconstruction process to produce a better result. The structure of the baby phantom can be seen clearly in the result of 3D ultrasound image reconstruction. However, the 3D reconstruction visualization required more advanced and complex computer software, which results in the 3D ultrasound cost more expensive than 2D ultrasound. Hence, the result of this research is to prove that the use of a low-cost device is able to produce 3D image convincingly. Figure 17 shows the 3D reconstructed image that is view from 86 multi-orientation ultrasound images.

The comparative studies between the baby phantom and the 3D reconstructed image were carried out by observing visible features of the baby phantom as shown in Figure 18. The 3D reconstruction of the head, hand, and abdomen of the 3D baby phantom images are indicated as the white colour part, which shown similarity with the targeted object. The results of reconstructed image are only able to show the general shape of the baby phantom as the ultrasound is unable to penetrate and move through the surface structure of baby phantom.

Some errors can be observed in the results of the 3D reconstructed image, such as the leg in reconstructed image is shorter than that of the baby phantom. This is due to the minor inaccuracy of position and orientation value during data acquisition step. Furthermore, the use of freehand scanning method in this research might cause some inaccuracy problem because some

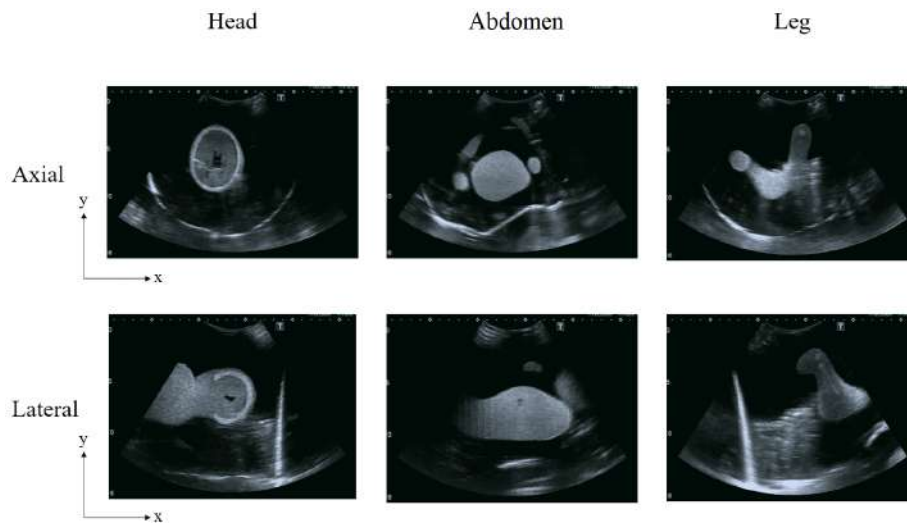


Fig. 16 2D ultrasound images taken by using ultrasound machine

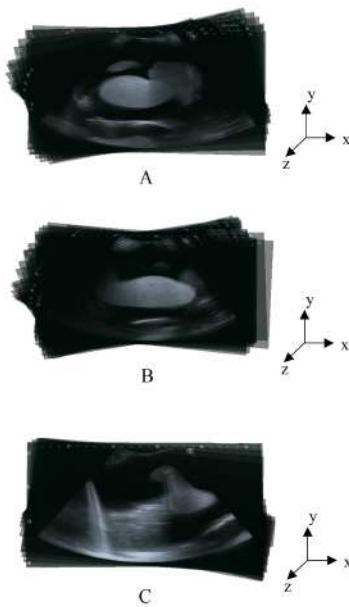


Fig. 17 3D image reconstructed view from 86 multiorientation ultrasound images in three part. (A) Head. (B) Body. (C) Leg.

parts of the baby phantom are not scanned by ultrasound probe. Hence, a good sweeping technique is required in order to cover all the baby phantom part. In addition to that, the number of frames taken also affects the 3D reconstructed images. The number of 2D ultrasound frames taken should be as many as possible so that it can cover most of the baby phantom area. Although this method can provide better visualization, the performance of the application might have diminished due to the large memory consumption in order to

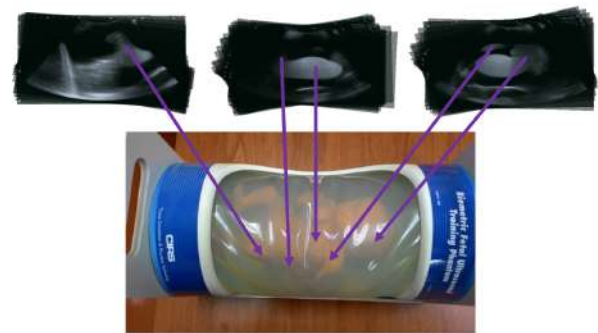


Fig. 18 3D image reconstructed view from 86 multiorientation ultrasound images

store and process the dataset during 3D reconstruction process.

Despite the minor error found in the result, the overall comparison shows the capabilities of low-cost devices, such as PS Move and PS Eye, in performing the 3D reconstruction works to illustrate a baby phantom shape.

## 5 Conclusion

In summary, the result shows that the low-cost game controller can be used to develop the position tracking system for 3D ultrasound reconstruction. The cost of the components and hardware used to build the system are able to keep to an absolute minimum. The systematic design of this system enables its implementation in any 2D ultrasound machine, thus provide some flexibility to the current ultrasound machine.

In order to improve the overall system, some future works are required as the following. First, the implementation of surface rendering method to visualize the 3D surface of the reconstructed images. Marching cubes algorithm is one of the popular surface rendering method, which produces a triangle mesh by computing iso-surface from discrete data [49], based on the intensity value from each 2D ultrasound images. Second, a good sweeping technique is required in order to cover all the region of interest.

Last but not least is the involvement of real human body part for the testing purpose. This study has shown the capability of the system with the use of baby phantom. It is recommended that further studies need to be carried out for bone scans and moving structures.

**Acknowledgements** This work is supported by the Fundamental Research Grant Scheme of Ministry of Education of Malaysia under the grant FRGS/1/2014/ICT07/UTM/03/1 and Research University Grant of Universiti Teknologi Malaysia Potential Academic Staff Grant QJ130000.2709.01K87.

## References

- Stephanie Sippel, Krithika Muruganandan, Adam Levine, and Sachita Shah. Review article: Use of ultrasound in the developing world. *International Journal of Emergency Medicine*, 4(1):72, 2011.
- C J Harvey, J M Pilcher, R J Eckersley, M J K Blomley, and D O Cosgrove. Advances in ultrasound. *Clinical Radiology*, 57(3):157–177, 2002.
- Andrew Gee, Richard Prager, Graham Treece, and Laurence Berman. Engineering a freehand 3D ultrasound system. *Pattern Recognition Letters*, 24(4-5):757–777, 2003.
- E De Fiori, C Rampinelli, F Turco, L Bonello, and M Bel-lomi. Role of operator experience in ultrasound-guided fine-needle aspiration biopsy of the thyroid. *La Radiologia medica*, 115(4):612–618, 2010.
- Dónal B. Downey, Aaron Fenster, and Jacqueline C. Williams. Clinical Utility of Three-dimensional US. *Radiographics*, 20(2):559–571, 2000.
- Aaron Fenster, Donal B Downey, and H Neale Cardinal. Three-dimensional ultrasound imaging. *Physics in Medicine and Biology*, 46(5):R67, 2001.
- Alexander Scharf, Marjan Farasaty Ghazwiny, Andrea Steinborn, Peter Baier, and Christof Sohn. Evaluation of two-dimensional versus three-dimensional ultrasound in obstetric diagnostics: A prospective study. *Fetal Diagnosis and Therapy*, 16(6):333–341, 2001.
- A. Gee, R. Prager, G. Treece, C. Cash, and L. Berman. Processing and visualizing three-dimensional ultrasound data. *British Journal of Radiology*, 77(SPEC. ISS. 2), 2004.
- S. Deb, B. K. Campbell, J. S. Clewes, and N. J. Raine-Fenning. Quantitative analysis of antral follicle number and size: A comparison of two-dimensional and automated three-dimensional ultrasound techniques. *Ultrasound in Obstetrics and Gynecology*, 35(3):354–360, 2010.
- T. Hata, H. Tanaka, J. Noguchi, and K. Hata. Three-dimensional ultrasound evaluation of the placenta. *Placenta*, 32(2):105–115, 2011.
- R. James Housden, Andrew H. Gee, Graham M. Treece, and Richard W. Prager. Sensorless reconstruction of unconstrained freehand 3D ultrasound data. *Ultrasound in Medicine and Biology*, 33(3):408–419, 2007.
- Andrew H. Gee, R. James Housden, Peter Hassenpflug, Graham M. Treece, and Richard W. Prager. Sensorless freehand 3D ultrasound in real tissue: Speckle decorrelation without fully developed speckle. *Medical Image Analysis*, 10(2):137–149, 2006.
- Aaron Fenster, Grace Parraga, and Jeff Bax. Three-dimensional ultrasound scanning. *Interface Focus*, 1(June):503–519, 2011.
- R. W. Prager, U. Z. Ijaz, A. H. Gee, and G. M. Treece. Three-dimensional ultrasound imaging. *Proceedings of the Institution of Mechanical Engineers, Part H: Journal of Engineering in Medicine*, 224(2):193–223, 2010.
- Honggang Yu, Marios S. Pattichis, Carla Agurto, and M. Beth Goens. A 3D Freehand Ultrasound System for Multi-view Reconstructions from Sparse 2D Scanning Planes. *BioMedical Engineering Online*, 10(1):7, 2011.
- Xiankang Chen, Tiexiang Wen, Xingmin Li, Wenjian Qin, Donglai Lan, Weizhou Pan, and Jia Gu. Reconstruction offreehand 3D ultrasound based on kernel regression. *BioMedical Engineering Online*, 13(1):124, 2014.
- Wolfgang Wein, Barbara Röper, and Nassir Navab. Integrating diagnostic B-mode ultrasonography into CT-based radiation treatment planning. *IEEE Transactions on Medical Imaging*, 26(6):866–879, 2007.
- Hui Zhang, Filip Banovac, Ralph Lin, Neil Glossop, Bradford Wood, David Lindisch, Elliot Levy, and Kevin Cleary. Electromagnetic tracking for abdominal interventions in computer aided surgery. In *Computer Aided Surgery*, volume 11, pages 127–136, 2006.
- Kevin Cleary and Terry Peters. Image-guided interventions: Review Technology and Clinical Applications. *Annual review of biomedical engineering*, 12:119–142, 2010.
- F. Khatib, S. Cooper, M. D. Tyka, K. Xu, I. Makedon, Z. Popovic, and D. Baker. Algorithm discovery by protein folding game players. *Proceedings of the National Academy of Sciences*, 108(47):18949–18953, 2011.
- Naofumi Kitsunezaki, Eijiro Adachi, Takashi Masuda, and Jun Ichi Mizusawa. KINECT applications for the physical rehabilitation. In *MeMeA 2013 - IEEE International Symposium on Medical Measurements and Applications, Proceedings*, pages 294–299, 2013.
- Stevie Giovanni, Yc Choi, Jay Huang, Et Khoo, and Kk Yin. Virtual Try-on using Kinect and HD camera. *Motion in Games SE - 6*, pages 55–65, 2012.
- S. W. Bailey and B. Bodenheimer. A comparison of motion capture data recorded from a Vicon system and a Microsoft Kinect sensor. In *Proceedings of the ACM Symposium on Applied Perception*, pages 121–121, 2012.
- Sehoon Ha, Yunfei Bai, and C. Karen Liu. Human motion reconstruction from force sensors. In *Proceedings of the 2011 ACM SIGGRAPH/Eurographics Symposium on Computer Animation - SCA '11*, pages 129–128, 2011.
- David Sindram, Iain H. McKillop, John B. Martinie, and David A. Iannitti. Novel 3-D laparoscopic magnetic ultrasound image guidance for lesion targeting. *HPB*, 12(10):709–716, 2010.
- Daniel F. Leotta, Paul R. Detmer, Odd Helge Gilja, Jing-Ming Jong, Roy W. Martin, Jean F. Primozich, Kirk W. Beach, and Eugene D. Strandness. Three-dimensional ultrasound imaging using multiple magnetic tracking systems and miniature magnetic sensors. In *Proceedings of*

- the IEEE Ultrasonics Symposium , volume 2, pages 1415–1418, 1995.
27. Masahiko Nakamoto, Kazuhisa Nakada, Yoshinobu Sato, Kozo Konishi, Makoto Hashizume, and Shinichi Tamura. Intraoperative magnetic tracker calibration using a magneto-optic hybrid tracker for 3-D ultrasound-based navigation in laparoscopic surgery. *IEEE Transactions on Medical Imaging* , 27(2):255–270, 2008.
  28. John E. Aldrich. Basic physics of ultrasound imaging, 2007.
  29. H Steiner, a Staudach, D Spitzer, and H Schaffer. Three-dimensional ultrasound in obstetrics and gynaecology: technique, possibilities and limitations. *Human reproduction (Oxford, England)* , 9(9):1773–1778, 1994.
  30. R. Salim, B. Woelfer, M. Backos, L. Regan, and D. Jurkovic. Reproducibility of three-dimensional ultrasound diagnosis of congenital uterine anomalies. *Ultrasound in Obstetrics and Gynecology* , 21(6):578–582, 2003.
  31. Fernando Bonilla-Musoles, Francisco Raga, and Newton G. Osborne. Three-dimensional ultrasound evaluation of ovarian masses. *Gynecologic Oncology* , 59(1):129–135, 1995.
  32. A. Kyei-Mensah, N. Maconochie, J. Zaidi, R. Pittrof, S. Campbell, and Seang Lin Tan. Transvaginal three-dimensional ultrasound: Reproducibility of ovarian and endometrial volume measurements. *Fertility and Sterility* , 66(5):718–722, 1996.
  33. Ketut E. Purnama, Michael H F Wilkinson, Albert G. Veldhuizen, Peter M A Van Ooijen, Jaap Lubbers, Johannes G M Burgerhof, Tri A. Sardjono, and Gijbertus J. Verkerke. A framework for human spine imaging using a freehand 3D ultrasound system. *Technology and Health Care* , 18(1):1–17, 2010.
  34. Duc V. Nguyen, Quang N. Vo, Lawrence H. Le, and Edmond H.M. Lou. Validation of 3D surface reconstruction of vertebrae and spinal column using 3D ultrasound data A pilot study. *Medical Engineering & Physics* , 37(2):239–244, 2015.
  35. T L Elliot, D B Downey, S Tong, C a McLean, and A Fenster. Accuracy of prostate volume measurements in vitro using three-dimensional ultrasound. *Academic radiology* , 3(5):401–406, 1996.
  36. Edward Leen, Senthil Kumar, Shahid A. Khan, Gavin Low, Keh Oon Ong, Paul Tait, and Mike Averkiou. Contrast-enhanced 3D ultrasound in the radiofrequency ablation of liver tumors. *World Journal of Gastroenterology* , 15(3):289–299, 2009.
  37. T Perl. Cross-platform tracking of a 6dof motion controller . PhD thesis, Vienna University of Technology, 2012.
  38. Dimitrios Ioannou, Walter Huda, and Andrew F. Laine. Circle recognition through a 2D Hough Transform and radius histogramming. *Image and Vision Computing* , 17(1):15–26, 1999.
  39. Derek Bradley and Gerhard Roth. Natural Interaction with Virtual Objects Using Vision-Based Six DOF Sphere Tracking Natural Interaction with Virtual Objects Using Vision-Based Six DOF Sphere Tracking. *Proceedings of the 2005 ACM SIGCHI International Conference on Advances in computer entertainment technology* , pages 19–26, 2005.
  40. Liang Dawei, Huang Qingming, Jiang Shuqiang, Yao Hongxun, and Gao Wen. Mean-shift blob tracking with adaptive feature selection and scale adaptation. *Proceedings - International Conference on Image Processing, ICIP* , 3:369–372, 2006.
  41. Dominique Boutet Roman Miletitch, Raphaël de Courville, Morgane Réboulard, Claire Danet, Patric Doan. Real-time 3D gesture visualisation for the study of Sign Language. *Electronic Workshops in Computing* , pages 275–280, 2012.
  42. Ken Shoemake. Animating rotation with quaternion curves. *ACM SIGGRAPH Computer Graphics* , 19(3):245–254, 1985.
  43. Daniel P. Skehan. Virtual retraining system for diagnostic ultrasound . PhD thesis, Worchester Polytechnic Institute, 2011.
  44. Min Xiu Kong, Chen Ji, Zheng Sheng Chen, and Rui Feng Li. Application of orientation interpolation of robot using unit quaternion. In *2013 IEEE International Conference on Information and Automation, ICIA 2013* , pages 384–389, 2013.
  45. Ole Vegard Solberg, Frank Lindseth, Lars Eirik Bø, Sebastian Muller, Janne Beate Lervik Bakeng, Geir Arne Tangen, and Toril A. Nagelhus Hernes. 3D ultrasound reconstruction algorithms from analog and digital data. *Ultrasonics* , 51(4):405–419, 2011.
  46. Robert Rohling, Andrew Gee, and Laurence Berman. A comparison of freehand three-dimensional ultrasound reconstruction techniques. *Medical Image Analysis* , 3(4):339–359, 1999.
  47. Thomas R. Nelson and Dolores H. Pretorius. Three-dimensional ultrasound imaging. *Ultrasound in Medicine & Biology* , 24(9):1243–1270, 1998.
  48. Dewi, D. E. O., T. L. R. Mengko, A. G. Purnama, I. K. E., Veldhuizen, and M. H. F. Wilkinson. An Improved Olympic Hole-Filling Method for Ultrasound Volume Reconstruction of Human Spine. *International Journal of E-Health and Medical Communications* , 1(3):28–40, 2010.
  49. Mahani Hafizah Wan, Kok Tan, and E Supriyanto. 3D ultrasound image reconstruction based on VTK. *Proceedings of the 9th WSEAS international conference on Signal processing* , pages 102–106, 2010.